

## Chapter XIII. Future Works

During the development of this thesis several other topics, besides those herein presented, have been analyzed. In some instances, these analyses have become a full research of a specific topic or they have turned into a subject matter of a future study. Among the reasons for not including those other subjects in this thesis are time constraints, opening new research topic areas beyond the scope of the present effort, and resource limitations to complete the analysis. Taking into account these grounds, the final scope of the present thesis was outlined leaving these related topics, also important, out of this manuscript. Despite this, efforts made in parallel to the development of the present work allowed the conclusion of some of these topics and the initiation of others. In order to be fair with the entire effort spent on (and/or triggered by) this research, the following paragraphs present in a brief manner those additional topics under the classification of “Future Works.” In particular, three areas of future contributions will be discussed; these are the application of electrical field, hydrodynamics near the electrode zone, and convective-dispersion analysis in electrodes and treatment zones.

In the area of applied electrical field, the role of geometrical dimensions in applications with axial and orthogonal (secondary) to flow electric fields was investigated using a rectangular capillary channel. In particular, the role of the applied orthogonal electrical field in controlling key parameters involved in the effective diffusivity and effective (axial) velocity of the solute were identified. Friendly mathematical relationships were obtained by applying the method of spatial (i. e., area) averaging to the solute species continuity equation; this was accomplished after the role of the capillary geometrical dimensions on the applied electrical field equations was studied. In fact, after this aspect was assessed, explicit analytical expressions were derived for the effective parameters, i.e., diffusivity and convective velocity as functions of the applied (orthogonal) electric field.

Previous attempts (Sauer et al., 1995) only lead to equations for these parameters that needed numerical solutions and, therefore, limited the use of such results to practical applications. These may include, for example, the design of new electrokinetic cell processes, electro-settlement in wastewater treatment as well as in process separation.

The dimensionless effective dispersion,  $\theta$ , and convective velocity,  $\hat{V}_{\text{eff}}$ , obtained in the analysis correspond to the following expression as functions of the applied (orthogonal) electric field.

$$\theta = \frac{1 - \hat{D}_{\text{eff}}}{\text{Pe}^2} = \frac{\Omega^4 \cdot e^\Omega + 360 \cdot \Omega + 60 \cdot \Omega^2 + 720 - \Omega^4 - 60 \cdot e^\Omega \cdot \Omega^2 - 720 \cdot e^\Omega + 360 \cdot \Omega \cdot e^\Omega}{5 \cdot \Omega^6 \cdot (1 - e^\Omega)} \quad (13.1a)$$

$$\hat{V}_{\text{eff}} = \frac{12 + 6 \cdot \Omega - 12 \cdot e^\Omega + 6 \cdot \Omega \cdot e^\Omega}{\Omega^2 \cdot (e^\Omega - 1)} \quad (13.1b)$$

These expressions above are explicit equations of the non-dimensional orthogonal field,  $\Omega$ , applied to the capillary and very useful to study the effect of this field on the effective transport parameters of the solute in the capillary channel. Equations 13.1 (a&b) may be useful in determining how secondary electrical field can aid in reducing the optimal separation time as illustrated in figure 13.1. This particular figure demonstrates the variation on the estimated time of separation of two hypothetical species, i.e. species A and B, whose ionic electro-mobility present reasonable differences under the stress of an orthogonal electric field. In addition, since the equations predicting the effective parameters show a direct dependence with the orthogonal electrical field, the implication on the separation time for optimal separation is easily (and clearly) determined. In other words, figure 13.1 presents the separation time,  $\tau$ , as a function of the applied dimensionless electrical field,  $\Omega_A$ , for different mobility ratios,  $u_B/u_A$ . As can be observed in the illustration the different curves present a minimum for the separation time,  $\tau$ , for a specific  $\Omega_A$  value. This minimum seems to be sensitive to the mobility ratio. For example, clearly for higher values of mobility ratios, the value of the minimum of the separation times decreases. On the other hand, smaller values of the mobility ratio will result in an increase of the minimum separation times.

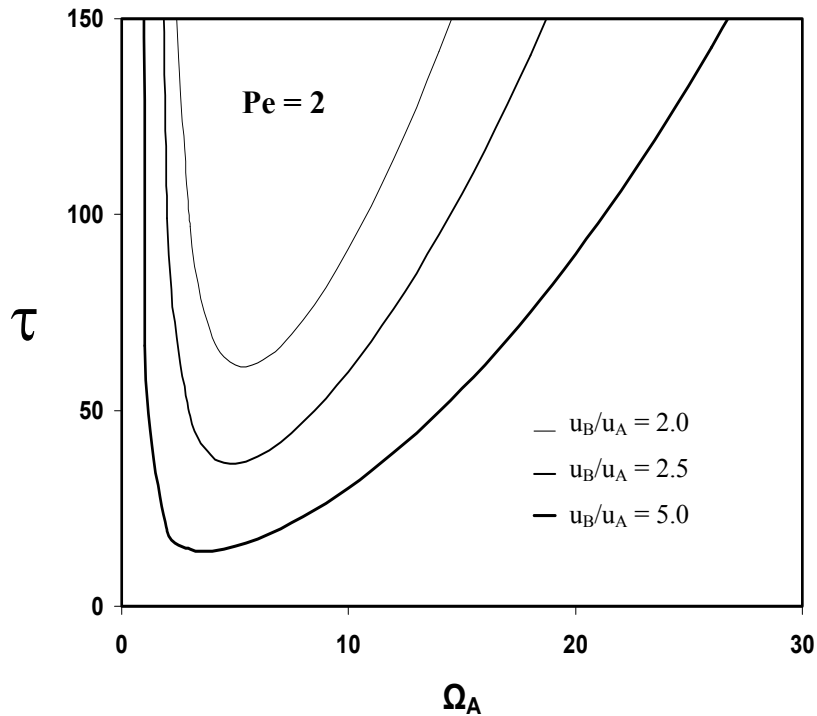


Figure 13.1 Time of separation for a resolution of two under Poiseuille flow regimes and orthogonal applied electric fields for  $Pe=2$  and different mobility ratio,  $u_B/u_A$ , values.

This contribution has been kept as a future work because, in essence, it introduces important modifications to the electroremediation process as until now conceived. The author believes that the results, partially presented here, will open new avenues of research in electrokinetic applications (Oyanader et al. 2003).

Similar to the above, in the topic of convective-dispersion and hydrodynamics near the electrode zone has been kept also as future work for the innovative ideas introduced to traditional electroremediation processes. In the approach, the method of spatial averaging is used in combination with the solute species continuity equation to determine the effect of Poiseuille and Couette type flows, under the stress of electric fields, on effective parameters, i.e., effective dispersion coefficient and effective convective velocity. Explicit analytical

expressions were derived for the effective parameters as a function of the applied electric field and flow regime ratios P and C, two new defined parameters that account for the Poiseuille and Couette type flows respectively. In particular, this approach focuses on modifying the operational function of traditional static electrodes to rotational devices where Couette type flows take place accelerating the dispersion of solute species and increasing the efficiency of the soil clean up process.

In this analysis, the resulting effective transport parameters (i.e. the dimensionless effective dispersion,  $\theta$ , and convective velocity,  $\hat{V}_{\text{eff}}$ ) obtained in the analysis correspond to the following expressions as functions of the applied secondary electric field:

$$\theta \equiv \frac{1 - \hat{D}_{\text{eff}}}{\text{Pe}^2} = P^2 \theta_P + PC \theta_{PC} + C^2 \theta_C \quad (13.2a)$$

where

$$\theta_P = \frac{\Omega^4 e^\Omega + 360\Omega + 60\Omega^2 + 720 - \Omega^4 - 60\Omega^2 e^\Omega - 720e^\Omega + 360\Omega e^\Omega}{5\Omega^6(1 - e^\Omega)} \quad (13.2b)$$

$$\theta_{PC} = \frac{-12 - 6\Omega - \Omega^2 + 12e^\Omega - 6\Omega e^\Omega + \Omega^2 e^\Omega}{6\Omega^3(e^\Omega - 1)} \quad (13.2c)$$

$$\theta_C = \frac{-24 - 12\Omega + \Omega^3 + 24e^\Omega - 12\Omega e^\Omega + \Omega^3 e^\Omega}{6\Omega^4(1 - e^\Omega)} \quad (13.2d)$$

and

$$\hat{V}_{\text{eff}} = 1 + P \hat{V}_{\text{eff}}^P + C \hat{V}_{\text{eff}}^C = P(1 + \hat{V}_{\text{eff}}^P) + C(1 + \hat{V}_{\text{eff}}^C) + \eta \quad (13.2e)$$

where

$$\hat{V}_{\text{eff}}^P = \frac{12 + 6 \cdot \Omega + \Omega^2 - 12e^\Omega + 6\Omega e^\Omega - \Omega^2 e^\Omega}{\Omega^2 \cdot (e^\Omega - 1)} \quad (13.2f)$$

$$\hat{V}_{\text{eff}}^C = \frac{2 + \Omega - 2 \cdot e^\Omega + \Omega e^\Omega}{\Omega \cdot (e^\Omega - 1)} \quad (13.2g)$$

The use of the obtained expressions for the effective transport parameters is similar to that already described on the previous example. However, this future work will highlight the

role that the electrodes may play in improving process efficiency if these devices can be designed with additional purpose other than just electrical conductors.

A third example deals with the hydrodynamics taking place near the electrode under Joule heating effect. The approach is similar to that of chapter IX, Electrodes of Rectangular Geometry; however the final solution of the system has been obtained analytically by a similarity type of solution. This analysis was not included in Part IV, Hydrodynamics Aspects of the Electrokinetic Remediation Process in the Near the Electrodes Zone, to do not introduce odd (biased) comparison between the analytical and numerical solutions. This is the reason why only numerical solutions were compared leaving the analytical solution for a future study.

The model system described by equations 9.25 a-d, differential in nature, can be solved analytically adopting a similarity type of solution for the source term,  $\phi^2$ , as a function of the axial coordinate. The analytical solution yields the following expressions for  $U^+$ , the dimensionless velocity amplitude in the  $\xi$ -direction (x-direction), and  $\delta^+$ , the dimensionless boundary layer thickness.

$$U^+ = \left[ \frac{420 \cdot J_1 + 4 \cdot \sqrt{11,025 \cdot J_1^2 + 35 \cdot \frac{Gr}{Re} \cdot (20 \cdot Re + 21)}}{(20 \cdot Re + 21)} \right] \cdot \xi^{1/2} \quad (13.3a)$$

$$\delta^+ = \left( \frac{420 \cdot J_1 + 4 \cdot \sqrt{11,025 \cdot J_1^2 + 35 \cdot \frac{Gr}{Re} \cdot (20 \cdot Re + 21)}}{80 \cdot (20 \cdot Re + 21)} - \frac{1}{2} \cdot J_1 \right)^{-1/2} \cdot \xi^{1/4} \quad (13.3b)$$

where

$$\phi^2 = J_1 \cdot \xi^{-1/2} \quad (13.3c)$$

For this future work, the most important figures are presented to illustrate the results yielded by the analytical solution.

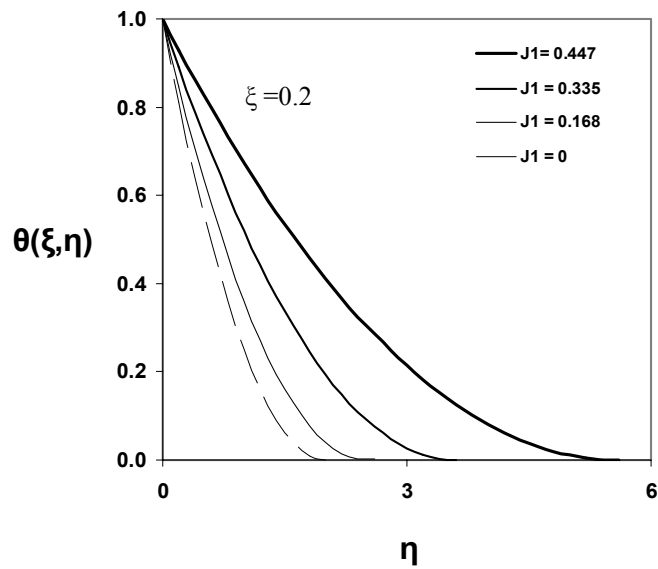


Figure 13.2 Dimensionless temperature profiles (inside the boundary layer) for various values of the heat generation parameter,  $J_1$ , and for the  $\eta$ -direction ( $\xi = 0.2$ ).

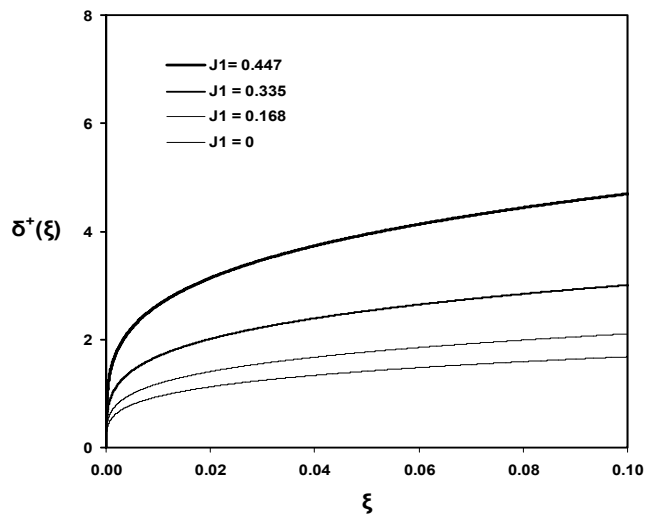


Figure 13.3 Dimensionless boundary layer thickness for different values of the heat generation parameter,  $J_1$ .

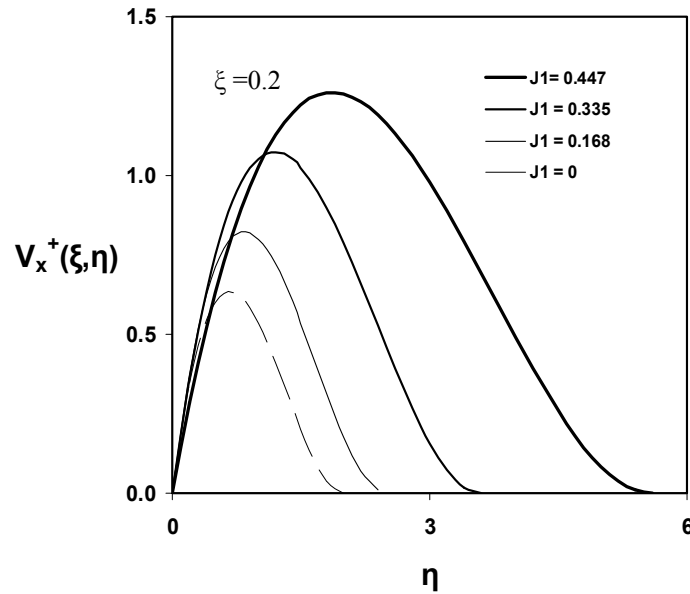


Figure 13.4 Dimensionless total velocity profiles showing the effect of the heat generation parameter,  $J_1$ , inside the boundary layer for the  $\eta$ -direction ( $\xi = 0.2$ ).

The analysis of figures 13.2, 13.3 and 13.4 is similar to those in chapter IX. To some extent, the forms of curve types are in agreement with the behavior predicted by the numerical solution. However, the main difference is that the source generation term,  $\phi^2$ , is not constant as in the numerical solution.

Finally, in the topic of convective-dispersion, a future contribution for which efforts were already initiated will report the effect of the three main driving forces, herein studies, on the transport parameters. In particular, the mixing dispersion will be analyzed using three geometrical aspects, i.e., rectangular, cylindrical and annular.